DOI: 10.1002/chem.200600717

Magnetic Face-to-Face Interaction and Electrocommunication in Chromium Sandwich Compounds

Christoph Elschenbroich,[c] Basil Kanellakopulos,[b] Frank H. Köhler,*[a] Bernhard Metz,[c] Rodrigue Lescouëzec,[a, e] Norbert W. Mitzel,[d] and Werner Strauß[a]

Abstract: The reaction of $[\{(C_5Me_5)CrCl_2\}_2]$ with [2.2](1,4)cyclophane gave $[(C_5Me_5)Cr\{[2.2](1,4)cyclophane\}]$ (**1**) and $[(C_5Me_5)Cr\{[2.2](1,4)cyclophane\}Cr(C_5Me_5)]$ (**2**), depending on the reaction conditions. X-ray structure analysis showed **2** to be a ministack which in turn is stacked in the lattice. The chromium atoms are 6.035 Å apart, and the distortion of the benzene rings to boat-shaped moieties is less pronounced than in parent [2.2](1,4)cyclophane. The NMR and EPR spectra were consistent with a $S=1/2$ ground state for **1** and with two interacting $S=1/2$ centers in **2**. Spin density was found in the ligand π systems, where its sign was negative when the π system was adjacent to chromium, while on the nonbonded benzene moiety of **1** it was positive. Cyclic voltammograms showed reductions to $\mathbf{1}^-$ and $\mathbf{2}^{2-}$, as well as oxidations to $\mathbf{1}^+$, $\mathbf{2}^+$, and $\mathbf{2}^{2+}$ which were quasireversible, whereas oxidations to $\mathbf{1}^{2+}$ and $\mathbf{2}^{3+}$ were irreversible. Interaction between the metal ions was revealed by a 260 mV separation of the redox waves belonging to $\mathbf{2}^+$, and $\mathbf{2}^{2+}$. Both cations were isolated as $[B(C_6H_5)_4]^-$ salts, which in solution decomposed to [2.2](1,4)cyclophane and $[(C_5Me_5)Cr\{(\eta^6\text{-}C_6H_5)B(C_6H_5)_3\}]$ (**3**). The ^1H and ^{13}C NMR spectra of **3** were in accordance with an $S=1$ ground state. Solid-state magnetic measurements of the dimetallic compounds showed antiferromagnetic interaction with $J=-122\ cm^{-1}$ for **2**, $J=-31\ cm^{-1}$ for $\mathbf{2}^+$ (ground state $S=1/2$), and $J=-23.5\ cm^{-1}$ for $\mathbf{2}^{2+}$ (with $H=-JS_1S_2$). The decrease of J in the series **2**, $\mathbf{2}^+$, and $\mathbf{2}^{2+}$ was traced to the number of unpaired electrons and, for the mixed-valent cation $\mathbf{2}^+$, to additional double exchange.

Keywords: chromium · electrochemistry · EPR spectroscopy · magnetic properties · sandwich complexes

Introduction

Flat molecules are intuitively thought to form stacks, at least in the solid state, thereby giving rise to face-to-face interactions. This is actually true when charge-transfer compounds are formed, for instance, the widely studied tetrathiafulvalene/tetracyanoquinodimethane derivatives.[1] Also, planar transition metal complexes deliberately adopt columnar structures as in the case of the tetracyanoplatinates,[2] or they do so by bifunctional donor links and covalent bridges, as known for metal phosphine, phthalocyanine, and other macrocyclic complexes.[3]

It occurred to us that, if such stacks can also be assembled from organometallic sandwich compounds and if each building block of the stack is an open-shell sandwich, varying magnetic interactions could be created. However, theoretical analyses[4] have shown that pillared stacks tend to be less stable than stepwise stacked geometries. Therefore, it is not surprising that molecule-derived pillars have been realized previously only in a combined organic/organometallic ap-

[a] Prof. Dr. F. H. Köhler, Dr. R. Lescouëzec, Dr. W. Strauß
Department Chemie
Technische Universität München
85747 Garching (Germany)
Fax: (+49) 89-2891-3762
E-mail: f.h.koehler@lrz.tu-muenchen

[b] Dr. B. Kanellakopulos
Forschungszentrum Karlsruhe
Hermann-von-Helmholz-Platz 1
76344 Eggenstein-Leopoldshafen (Germany)

[c] Prof. Dr. C. Elschenbroich, Dr. B. Metz
Fachbereich Chemie
Philipps-Universität Marburg
Lahnberge, 35043 Marburg (Germany)

[d] Prof. Dr. N. W. Mitzel
Institut für Anorganische und Analytische Chemie
Corrensstrasse 30, 48149 Münster (Germany)

[e] Dr. R. Lescouëzec
New address:
Laboratoire de Chimie Inorganique et Matériaux Moléculaires
UMR CNRS 7071, Université Pierre et Marie Curie
4 Place Jussieu, 75252 Paris Cedex 05 (France)

Supporting information for this article is available on the WWW under http://www.chemeurj.org/ or from the author.

proach, that is, in charge-transfer salts consisting of electron-poor π compounds and electron-rich sandwich molecules.[5] By contrast, pure neutral π compounds like naphthalene[6] avoid pillar stacking, and even the arrangement of naphthalene radical cation[7] and anion[8] in the lattice would favor very little if any face-to-face interaction.

It follows that the face-to-face geometry of π complexes must be forced, and this has been realized for cyclopentadienyl-derived species by anchoring them at the 1,8 positions of naphthalene (see **A** in Scheme 1).[9,10] When the

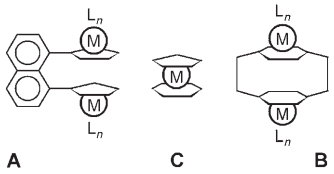

Scheme 1.

bridge is more flexible, parallel orientation of the π ligands tends to be avoided.[11] To force such a geometry we chose the cyclophane approach, which has been documented for diamagnetic metal compounds[12a] (see **B** in Scheme 1), while a broader view on cyclophanes was given recently.[12b] The desired unpaired spins were introduced by formally linking the $S=1/2$ sandwich (benzene)cyclopentadienylchromium[13] (see **C** in Scheme 1 with M = Cr) with ethylene groups. The resulting compound was expected to be a model for the study of ionic charge and magnetic interactions between paramagnetic sandwich compounds at short distance.

Results and Discussion

Syntheses of (C_5Me_5)Cr[2.2](1,4)cyclophane derivatives: (Pentamethylcyclopentadienyl)chromium(arene) derivatives are generally accessible by first generating a reactive species containing the (C_5Me_5)Cr fragment, and then transferring this fragment to an arene.[14] The most convenient starting material is $[\{(C_5Me_5)CrCl_2\}_2]$,[15] and therefore the synthesis of (C_5Me_5)Cr(arene) compounds consists of successive (C_5Me_5)Cr-transfer and reduction steps. First, the reactivity of $[\{(C_5Me_5)CrCl_2\}_2]$ is increased by addition of anhydrous aluminum halide, which labilizes the Cr–Cl bonds and splits the dinuclear compound. Subsequently, in the presence of an arene and aluminum, the cation $[(C_5Me_5)Cr(arene)]^+$ is formed, which is further reduced to the neutral compound by reduction with $LiAlH_4$. When this was done by heating a mixture of $AlCl_3$, [2.2](1,4)cyclophane, and Al as reducing agent, no (C_5Me_5)Cr(arene)-type compound could be isolated, although the procedure had been successful for benzene and substituted congeners.[14] In retrospect, this must be ascribed to the particular bonding between chromium and [2.2](1,4)cyclophane (see below), which renders the target molecule thermally labile. When milder conditions were chosen (reaction in refluxing cyclohexane rather than in a melt of $AlCl_3$ and $AlBr_3$) only one (C_5Me_5)Cr fragment could be bonded to [2.2](1,4)cyclophane, and **1** (see Scheme 2) was obtained in analytically pure form, albeit in low yield.

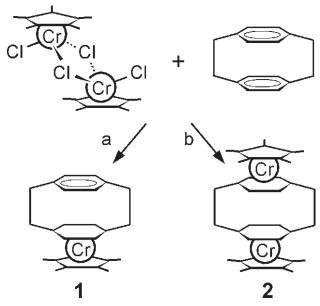

Scheme 2. Synthesis of [2.2](1,4)cyclophane chromium derivatives. a) $AlCl_3/AlBr_3/Al$, $LiAlH_4$; b) $LiAlH_4/AlEt_3$.

When the (C_5Me_5)Cr fragment was generated via a supposed (C_5Me_5)Cr(alkyl)hydride species by using $AlEt_3$ and $LiAlH_4$, the reaction proceeded slowly at ambient temperature. After workup red needles of **2**·THF were obtained from THF solution in 60% yield, while solvent-free needles of **2** formed after recrystallization from benzene. The presence of THF in the crystal was established by elemental analysis and the NMR spectra of **2**·THF in C_6D_6.

In the mass spectrometer **1** and **2** readily underwent chromium–arene cleavage. Thus $[\mathbf{1}^+]$ appeared only at low abundance, while $[\mathbf{2}^+]$ or $[\mathbf{2}^{2+}]$ was not detected. Rather, the base peak of both compounds was $C_8H_8^+$ resulting from fragmentation of the charged [2.2](1,4)cyclophane ligand.[16] This is in line with the fact that **1** and **2** do not melt but decompose on heating.

Crystal structure of compound 2: Slow solvent evaporation of a concentrated solution of **2** in benzene yielded red needles suitable for X-ray analysis. The molecular structure of **2** (Figure 1) can be regarded as a ministack in which two chromium atoms are sandwiched symmetrically between four π-ligand planes. The chromium atoms are separated by 6.035 Å, and the two benzene faces of the (C_5Me_5)Cr(benzene) moieties have a mean distance of only 2.838 Å (between the unweighted centroids) as well as 2.695 Å for C1···C1′ and C4···C4′. This means that the benzene rings adopt a boat conformation with interplanar angles of 8.8° and 8.2° for C2C1C6–C2C3C5C6 and C3C4C5–C2C3C5C6, respectively. In addition, the bonds C1–C7 and C4–C8 are bent away from chromium and out of the planes C2C1C6 and C3C4C5 by 10.6 and 14.7°, respectively. Compared to parent [2.2](1,4)cyclophane,[17] as a ligand in **2** the cyclophane is less distorted. Generally, π complexation of [2.2](1,4)cyclophane occurs in two separate steps, as exemplified by the mono-$Cr(CO)_3$[18a,b] and bis-$Cr(CO)_3$[18a] derivatives. This is assisted by the relief of antibonding π–π interaction between the clamped benzene moieties on *exo* coordination.[18b] Compound **2** seems to have the shortest separation

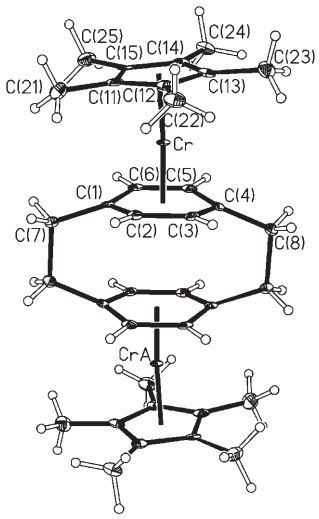

Figure 1. Molecular structure of **2**. Selected bond lengths [Å] and angles [°]: Cr–C(1) 2.178(2), Cr–C(2) 2.102(2), Cr–C(6) 2.102(2), Cr–C(5) 2.119(2), Cr–C(3) 2.119(2), Cr–C(11) 2.154(2), Cr–C(12) 2.157(2), Cr–C(13) 2.159(2), Cr–C(15) 2.161(2), Cr–C(14) 2.166(2), Cr–C(4) 2.215(2), C(1)–C(2) 1.423(3), C(1)–C(6) 1.429(3), C(1)–C(7) 1.512(3), C(2)–C(3) 1.421(3), C(3)–C(4) 1.426(3), C(4)–C(5) 1.421(4), C(4)–C(8) 1.509(3), C(5)–C(6) 1.420(3), C(7)–C(8′) 1.607(3); C(2)-C(1)-C(6) 119.1(2), C(3)-C(2)-C(1) 119.9(2), C(11)-C(12)-C(13) 108.0(2), C(14)-C(13)-C(12) 107.8(2). Symmetry transformations used to generate equivalent atoms: $-x+1$, $-y$, $-z+2$.

between six-membered rings known so far. The distance of the chromium atom from the mean five-membered ring plane C11–C15 is 1.783 Å, while that from the benzene plane C2–C6 is 1.564 Å. The ministacks are slightly bent, as can be seen from an angle of 5.5° between the planes just mentioned.

In the lattice, compound **2** is arranged in columns which are oriented along the bisector of the angle β of the unit cell (Figure S1a). The column cores are isolated from each other by the methyl groups of the C_5Me_5 ligands and the ethylene linkers of the cyclophanes. Within the columns the C_5Me_5 planes of adjacent molecules are separated by 3.787 Å and strongly slipped relative to each other (Figure S1b). Whether this entails overlap of the corresponding π orbitals is an issue of the magnetic studies below.

NMR and EPR spectra of compounds 1 and 2: Molecules of the type $(C_5Me_5)Cr(arene)$ belong to the relatively rare paramagnetic species which have an intermediate electron-spin relaxation rate, so that magnetic resonance spectroscopy can be shifted into both the NMR and the EPR regimes by changing the temperature.

The ^{1}H NMR spectrum of **1** in Figure 2 shows three broad signals whose shifts were temperature-dependent, as expected for a paramagnetic compound. The signal shifts relative to diamagnetic standards (see Experimental Section), that is, the paramagnetic shifts caused by the unpaired electron spin density at 305 K, were $\delta^{para}_{305}(CH_3)=13.6$ ppm, $\delta^{para}_{305}(CH_2)=4.4$ ppm, and $\delta^{para}_{305}(C_6H_4)=-7.6$ ppm. The last two signals must belong to the protons of that part of [2.2](1,4)cyclophane which is not bonded to chromium, because for the other benzene and CH_2 moieties the signals should appear near $\delta=260$ and -60 ppm, respectively.[14] The assignment was based on the relative signal areas and the fact that for dipolar relaxation the signal half-width is proportional to r^{-6} where r is the Cr···H distance. From the analogous structure of **2** it is known that the distances of Cr from the C_6H_4 and CH_2 protons are 5.07 and 5.28 Å, respectively. Hence, the latter protons should have the narrower signal. Neither for **1** nor for **2** could the other CH_2 and C_6H_4 signals be detected near $\delta=260$ and -60 ppm, respectively. We ascribe this to the fact that **1** and **2** are not very soluble and that the half-widths of the arene proton signals of similar compounds are in the range of 5 kHz[14] so that, in the present case, they disappear in the noise. Correspondingly, for **2** just the signal of the C_5Me_5 ligand (δ^{para}_{305} $(CH_3)=-12.7$ ppm) appeared.

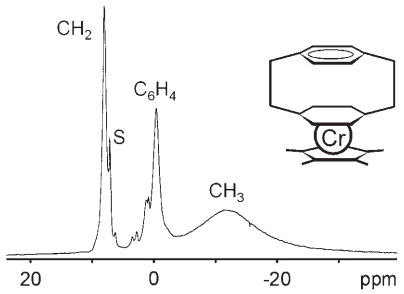

Figure 2. ^{1}H NMR spectrum of **1** in C_6D_6 at 305 K. The assignments C_6H_4 and CH_2 refer to the noncoordinated part of [2.2](1,4)cyclophane; S = solvent; scale relative to TMS.

The liquid-solution EPR spectrum of **1** (Figure 3, top) consists of a quintet centered at $g=1.9890$ which shows an isotropic hyperfine coupling of $A(^1H)_{iso}=0.406$ mT with four equivalent protons. This confirms that one of the benzene

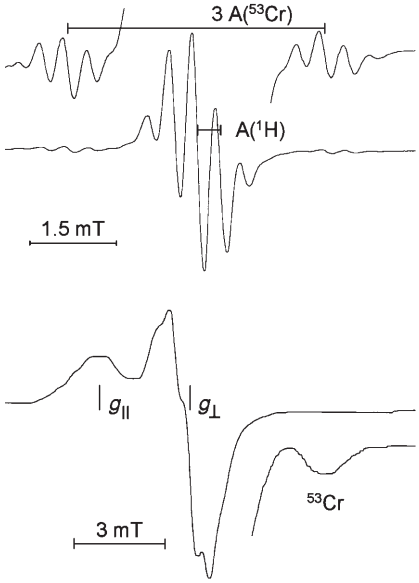

Figure 3. EPR spectra of **1** dissolved in toluene. Top: Liquid solution at −90 °C; ^{53}Cr satellites amplified 10×. Bottom: Solid solution at −160 °C.

rings of [2.2](1,4)cyclophane is bonded to chromium. As can be calculated from the NMR data given above, the hyperfine couplings with the other protons must be smaller than 0.02 mT, and hence they were not resolved in the EPR spectrum. In addition, two components of a satellite quartet are visible, which originates from hyperfine interaction with the ^{53}Cr isotope ($I=3/2$, natural abundance 9.5%) and yields $A(^{53}Cr)_{iso}=1.500$ mT. Compared to the hyperfine data of simpler $(C_5Me_5)Cr(arene)$ compounds ($A(^1H)_{iso}\approx 0.490$ mT, $A(^{53}Cr)_{iso}=1.40$ mT),[14,19] in **1** the hyperfine coupling to chromium is stronger, while that to the ligand protons is weaker. An even larger hyperfine interaction ($A(^{53}Cr)_{iso}=1.85$ mT) has been observed for chromium *exo*-bonded to two [2.2](1,4)cyclophane ligands.[20] This is in line with weaker metal bonding of the doubly folded benzene ring of [2.2](1,4)cyclophane.

According to the solid-solution EPR spectrum (Figure 3, bottom) **1** appears as an axial molecule, because two of the three expected *g* components are not resolved. The relevant data are $g_\parallel=2.0013$, $g_\perp=1.9835$, $\langle g\rangle=1.9894$, $A(^1H)_\parallel=0.192$ mT, $A(^1H)_\perp=0.513$ mT, $\langle A(^1H)\rangle=0.406$ mT, $A(^{53}Cr)_\parallel=0.033$ mT, $A(^{53}Cr)_\perp=2.233$ mT, and $\langle A(^{53}Cr)\rangle=1.500$ mT. The most striking deviation from the data of undistorted $(C_5Me_5)Cr(arene)$ derivatives[14] is the much smaller $A(^1H)_\parallel$ value, while $A(^1H)_\perp$ is hardly affected. With the reasonable assumption that the *g* tensor is aligned along the main axis of **1**, this confirms the conclusion that the bent benzene ring of [2.2](1,4)cyclophane experiences weaker bonding to chromium. In addition, the data show that the unpaired electron of **1** is located in an MO with predominately d_{z^2} character.[14,19a,21]

The liquid-solution EPR spectrum of **2** consists of a broad unstructured absorption with a superimposed quintet signal. The splitting of the latter signal equals that observed for **1** and attests to ready cleavage of the binuclear complex **2** in solution. The fact that for **2** no hyperfine structure is detectable points to a fairly strong exchange interaction (see below) which accelerates spin–spin relaxation and broadens the hyperfine components. The same behavior is displayed by the triplet radical cation $[(H_5C_6{-}C_6H_5)_2Cr_2]^{2+}$, in which two d^5 chromium sandwich cations are linked in a parallel rather than a face-to-face arrangement.[22]

The solid-solution EPR spectrum of **2** (Figure 4) is characteristic of a triplet radical with features centered near $g=2$ and $g=4$ for the $\Delta M_s=\pm1$ and $\Delta M_s=\pm2$ transitions, respectively. In addition, in the center near $g=2$ there is a signal with $g=1.984$, which is assigned to $g_\perp$ of $(C_5Me_5)Cr^I$ species with $S=1/2$. Such species are formed when **2** loses a $(C_5Me_5)Cr$ fragment to give **1**. Actually, the EPR spectra slowly change with time: the feature at $g=1.984$ increases at the expense of all other signals. This corresponds to the mass spectral behavior of **2** and its easy decomposition on heating. The signal of the $S=1/2$ species appears rather big, because each molecule of **2** decomposes to give two $S=1/2$ species. Also, from the magnetic data (see below) it follows that at low temperature the $S=1$ state of **2** is little populated: at −156 °C we see only 18% of **2**.

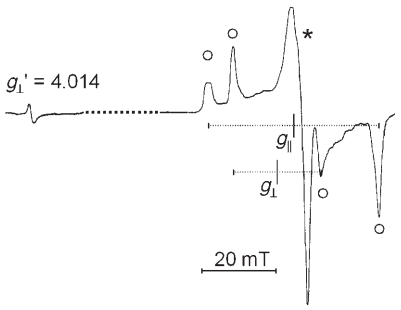

Figure 4. Solid-solution EPR spectrum of triplet radical **2** (○) and its monoradical decomposition product (*) in toluene at −156 °C.

The $\Delta M_s=\pm1$ part of the spectrum of **2** consists of four signals due to the splitting of the *g* factors which occurs because of the dipole interaction of the unpaired spins at each chromium atom. As **2** is a centrosymmetric molecule the analysis is straightforward and yields $g_\parallel=2.0023$, $g_\perp=2.0311$, and an axial zero-field splitting of $D=2.14\times10^{-2}$ cm^{-1}. Within the error limits the spacing of the $g_\perp$ components is twice that of the $g_\parallel$ components so that the nonaxial zero-field splitting *E* is zero. Hence, from the EPR point of view **2** is an axial molecule like **1**. In the $\Delta M_s=\pm2$ part of the spectrum of **2** only one component, $g'_\perp=4.014$, appears as expected for an axial triplet radical. For ideal dipolar electron spin coupling the zero-field splitting is related to the distance *r* between spin centers by[23] $r=[(\beta^2/3D)(2g_\parallel^2+g_\perp)]^{1/3}$, where β is the Bohr magneton. For compound **2** $r=4.34$ Å is obtained, which must be compared with the Cr–Cr separation of 6.035 Å from crystal structure analysis. It follows that here the simple point-dipole treatment of the coupling is not applicable, because spin transfer to the ligands (evident from the NMR, EPR, and magnetic results) means that the unpaired electrons are not fully localized at the chromium atoms (see below). Interestingly, for the parent [2.2](1,4)cyclophane triplet radical a much larger *D* value of 0.1079 cm^{-1} (and splitting of $g_\perp$) has been reported.[24] This qualitatively fits the reasoning, because here the radical centers are much closer together than in **2**. However, the calculated distance (≈2.5 Å) is again too short because of spin delocalization.

It seems appropriate to interpret compound **1** as a [2.2](1,4)cyclophane radical having a reduced-spin source and to compare it with the parent [2.2](1,4)cyclophane radical anion, which has been studied most intensively by Gerson.[25] In the latter anion the unpaired electron is fully delocalized when it exists as a solvent-separated ion pair and the spin distribution is represented by the singly occupied benzene e_{2g}-type orbital shown in Figure 5. To unify the discussion, the D_{6d} symmetry labels are used, while the degeneracy of all e-type orbitals is actually lifted. When contact ion pairs are formed, for instance, with K^+, Coulomb interaction shifts the charge and hence the spin density toward the counterion, and this is reflected by the proton hyperfine coupling constants (Figure 5, top left). In compound **1** the situation is quite different. The unpaired elec-

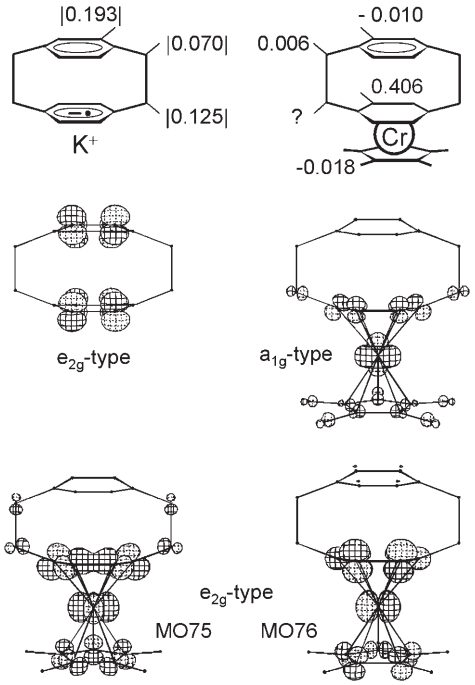

Figure 5. Proton hyperfine coupling constants [mT] of the potassium salt of [2.2](1,4)cyclophane radical anion in THF at 178 °C[24] and of compound **1**. Also shown are the respective wave functions (without H atoms) of interest for the discussion of the spin distribution.

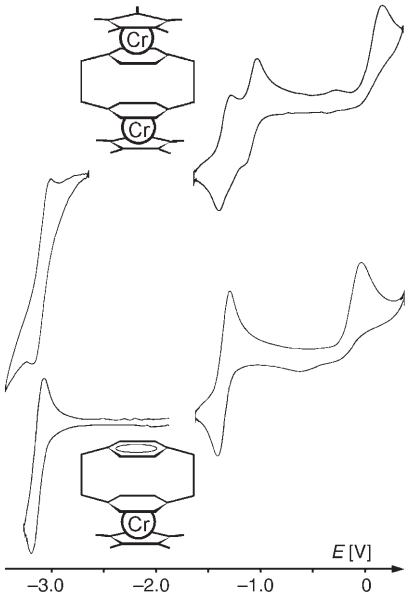

Figure 6. Cyclic voltammograms of **1** (bottom) and **2** (top) in THF at 22 °C and 200 mV s^{-1}. Scale relative to the couple $[Cp_2Fe]/[Cp_2Fe]^+$.

tron occupies an a_{1g} orbital, and spin density appears in the ligands as described in detail for $[(C_5Me_5)Cr(C_6H_6)]$ in the Supporting Information. In particular, the six-membered ligand receives more spin than the five-membered one, so that the distance between spin centers calculated from the point-dipolar model mentioned above appears shorter than the experimental Cr···Cr distance. The dominant spin delocalization mechanism is the polarization of bonding electrons in the e_{2g} orbitals (MOs 75 and 76 in Figure 5), while the a_{1g} orbital contributes some direct spin delocalization. In any case, much less spin is transmitted from chromium to the remote benzene ring than in the [2.2](1,4)cyclophane radical anion. This is confirmed by the proton hyperfine coupling constants $A(^1H)$ of **1** (Figure 5, top right) obtained from the EPR and NMR spectra. In addition, the signs of $A(^1H)$ are available from NMR spectroscopy. Going back from the benzene protons to the benzene core is associated with inversion of the spin sign (through C−H bond polarization). Hence, the overall result is that the spin density induced in the π systems of the benzene rings adjacent to and remote from the chromium atom is negative and positive, respectively. These conclusions are useful for understanding the magnetic interaction presented below.

Redox chemistry of compounds 1 and 2: The cyclic voltammograms (CVs) of **1** and **2** indicated that both compounds can be reduced and oxidized. As shown by representative CVs in Figure 6 compound **1** underwent electron transfers (ETs) to the monoanion at a half-wave potential of $E_{1/2}=-3.01$ V (peak potential separation $\Delta E_p=118$ mV, ratio of cathodic and anodic peak currents at a scan rate of 200 mV s^{-1} $i_{pc}/i_{pa}=0.83$) and to the monocation at $E_{1/2}=-1.27$ V ($\Delta E_p=116$ mV, $i_{pc}/i_{pa}=0.75$). As indicated by ΔE_p both ETs were electrochemically quasireversible, much in the same way as the ET of ferrocene, which was added for potential referencing. In THF both the resulting cation and anion were not perfectly stable, as followed from $i_{pc}/i_{pa}<1$ and the fact that this ratio increased with scan rate. In addition, a chemically irreversible oxidation to the dication occurred with an anodic peak at $E_{pa}=-0.05$ V. For the reduction a [2.2](1,4)cyclophane-centered ET can be excluded, because on the $[Cp_2Fe]/[Cp_2Fe]^+$ scale and in THF $E_{1/2}\approx-3.6$ V would be expected.[26] It turns out that compound **1** is oxidized at almost the same potential (−1.27 V) as $[(C_5Me_5)Cr(C_6Me_6)]$ (−1.24 V), while $[(C_5Me_5)Cr(C_6H_6)]$ is oxidized at −0.86 V.[14] Hence, irrespective of different solvation effects, it looks as if the [2.2](1,4)cyclophane ligand behaves like an electron-rich arene. This is not true, because photoelectron data clearly demonstrate that through-bond and through-space interactions with the second benzene ring are much more important than substitution effects.[27] The CV of **2** showed two ETs near −1.2 V, as expected for successive oxidation of the two interacting metal centers. From the ET values of $E_{1/2}(A)=-1.08$ V ($\Delta E_p=120$ mV) and $E_{1/2}(B)=-1.34$ V ($\Delta E_p=115$ mV) an ET separation of $\Delta E_{1/2}=260$ mV is calculated for the steps $Cr^I\rightarrow Cr^{II}$. This establishes efficient communication between the charges at the chromium atoms.

The reduction at $E_{1/2}=-2.99$ V ($\Delta E_p=180$ mV) is interpreted as two unresolved ETs to chromium(0) centers, because the peak current difference is close to the sum of those of $E_{1/2}(A)$ and $E_{1/2}(B)$. The irreversible oxidation to

chromium(III) centers at $E_{pa} = 0.15$ V gives no hint to the transfer of two electrons.

The redox chemistry of transition metal [2.2](1,4)cyclophane compounds has been investigated thoroughly for Fe[28] and Ru.[29] Structurally most similar to compounds **1** and **2** are the diamagnetic cations $[(C_5H_5)Fe\{[2.2](1,4)cyclophane\}]^+$ and $[(C_5R_5)Fe\{[2.2](1,4)cyclophane\}Fe(C_5R_5)]^{2+}$. Geiger et al. showed that on reduction the compounds suffer cleavage of the Fe–arene bond, due to the fact that the benzene moieties are not planar. Our CV observations on **1** and **2** parallel these findings for the Cr^{II} species even though another electronic ground state is engaged. In view of further chemistry we were most interested in the redox potential splitting of the dimetallic compounds. For the iron compounds $\Delta E_{1/2} = 140$ mV was found when the terminal ligand was C_5H_5,[28a] while for C_5Me_5 Astruc et al.[28b] could not resolve different ETs. This means that the intermediate $Fe^{I/II}$ mixed-valent species is (rather) unstable. The propensity of a mixed-valent compound to undergo redox disproportionation can be determined with the equation[30] $K = \exp(-\Delta E_{1/2}F/RT)$, where K is the equilibrium constant, F the Faraday constant, and T the absolute temperature. In the case of a solution of **2** in THF, the ET separation of 260 mV predicts that at 298 K only 8% of the $Cr^{I/II}$ species would be converted to $Cr^{I/I}$ and $Cr^{II/II}$. Because $[(C_5R_5)Cr(arene)]^+$ cations are more stable in 1, 2-difluorobenzene,[14] this solvent was chosen for the reaction of **2** with $[(C_5Me_5)_2Fe]^+[B(C_6H_5)_4]^-$. Addition of one and two equivalents of the oxidant immediately gave brown and orange powders, respectively, which were insoluble in nonpolar solvents. Elemental analyses established that the orange product was pure $\mathbf{2}^{2+}[B(C_6H_5)_4]^-_2$, which crystallized with one solvent molecule per formula unit, while the brown powder was $\mathbf{2}^{+}[B(C_6H_5)_4]^-\cdot 0.1\,C_6H_4F_2$. In both cases 1,2-difluorobenzene could not be removed by prolonged washing with hexane.

Attempts to record NMR spectra from the powders dissolved in polar solvents like CD_2Cl_2 and 1,2-difluorobenzene resulted in decomposition. About one hour after sample preparation big and small proton signals were observed between −10 and −20 ppm, and the small signals further decreased with time. When starting from $\mathbf{2}^{2+}[B(C_6H_5)_4]^-_2$ the free ligand [2.2](1,4)cyclophane could be isolated. In addition, orange-red zwitterionic compound **3** formed (Scheme 3), which had been obtained previously in 33% yield by treating $[(C_5Me_5)Cr(thf)_2(CH_3)]^+[B(C_6H_5)_4]^-$ with styrene in CH_2Cl_2.[31] Formation of **3** is not restricted to the

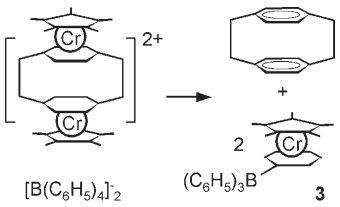

Scheme 3. Decomposition of $\mathbf{2}^{2+}[B(C_6H_5)_4]^-_2$ in CH_2Cl_2

precursor $\mathbf{2}^{2+}[B(C_6H_5)_4]^-_2$. Thus, after dissolving $[(C_5Me_5)Cr(C_6H_6)]^+[B(C_6H_5)_4]^-$[14] in CH_2Cl_2 **3** was isolated in (unoptimized) 51% yield.

The ^{1}H NMR spectrum of **3** in Figure 7 is characteristic of a paramagnetic compound. The comparison of more detailed ^{1}H and ^{13}C NMR data with those of $[(C_5Me_5)Cr(arene)]^+$ ions (see Supporting Information) establishes two unpaired electrons, negative spin density in both ligand π systems, and little spin transmission to the uncoordinated phenyl groups of the $[B(C_6H_5)_4]^-$ ligand.

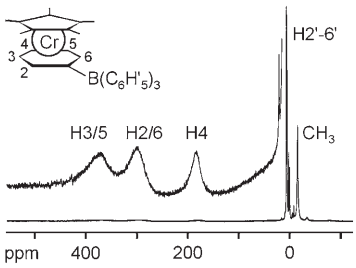

Figure 7. ^{1}H NMR spectrum of compound **3** in $[D_8]$THF at 305 K; the signals of H2–H6 are amplified.

Magnetic properties of the dinuclear chromium cyclophane compounds: The magnetic susceptibilities of polycrystalline samples of **2**, $\mathbf{2}^{+}[B(C_6H_5)_4]^-\cdot 0.1\,C_6H_4F_2$, and $\mathbf{2}^{2+}[B(C_6H_5)_4]^-_2\cdot C_6H_4F_2$ were measured in the temperature ranges 1.3–296 K, 1.3–306 K, and 1.3–293 K, respectively (Figure 8). At 295.5 K, **2** has a $\chi_m T$ value of

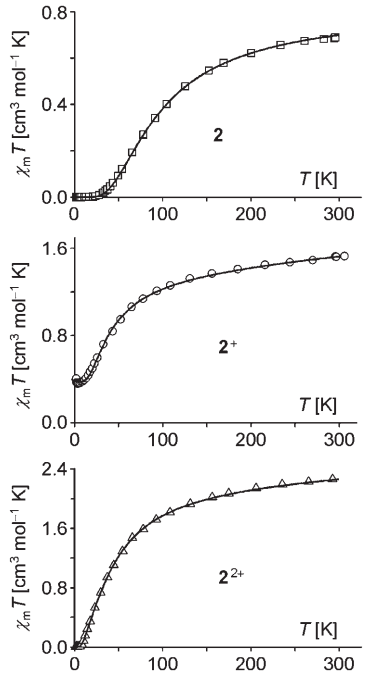

Figure 8. Temperature dependence of $\chi_m T$ of the dinuclear chromium compounds **2** (top) and the $[B(C_6H_5)_4]^-$ salts of $\mathbf{2}^{+}$ (center) and $\mathbf{2}^{2+}$ (bottom). The solid lines are best-fit curves.

0.689 $cm^3 mol^{-1} K$ which is smaller than the value expected for two isolated Cr^I $S=1/2$ centers (0.75 $cm^3 mol^{-1} K$ assuming $g=2$) and which points to antiferromagnetic interaction (Figure 8, top). Indeed, with deceasing temperature the characteristic nonlinear decrease of $\chi_m T$ is seen, below 10 K the $S=0$ spin ground state is reached, and the sample is virtually diamagnetic. For compound $\mathbf{2}^+[B(C_6H_5)_4]^- \cdot 0.1\,C_6H_4F_2$ the χ_{mT} value of 1.527 $cm^3 mol^{-1} K$ at 306 K slightly exceeds what is expected for the spin-only value of independent Cr^{II} $S=1$ and Cr^I $S=1/2$ centers (1.375 $cm^3 mol^{-1} K$ assuming $g=2$). According to the χ_{mT}/T curve (Figure 8, center) antiferromagnetic interaction is again effective, but in this case a plateau of 0.4 $cm^3 mol^{-1} K$ is reached below 10 K. This corresponds to the $S=1/2$ ground state expected for the mixed-valent cation $\mathbf{2}^+$. Finally, for $\mathbf{2}^{2+}[B(C_6H_5)_4]^-_2 \cdot C_6H_4F_2$ the $\chi_m T/T$ curve (Figure 8, bottom) is similar to that of antiferromagnetic **2**, except that at 292.6 K a $\chi_m T$ value of 2.263 $cm^3 mol^{-1} K$ was measured in accordance with the spin-only value of two independent Cr^{II} $S=1$ centers. The Hamiltonian appropriate for the interaction is $H=-JS_1S_2$ where J is the exchange coupling constant and S_1 and S_2 are the spins at the two chromium atoms. Fitting the data of **2** and the salts of $\mathbf{2}^+$ and $\mathbf{2}^{2+}$ to Equations (1a–c), respectively, gave the data collected in Table 1.

Table 1. Fitting parameters for the exchange coupling of the dinuclear chromium compounds.

	2	$\mathbf{2}^{+}$[a]	$\mathbf{2}^{2+}$[b]
S_1, S_2	1/2, 1/2	1, 1/2	1, 1
J [cm^{-1}]	−122	−31	−23.5
g	2.08	2.07 (Cr^I) 2.01 (Cr^{II})	2.15
TIP [$cm^3 mol^{-1} K$]	39×10^{-6}	548×10^{-6}	385×10^{-6}
R[c]	5.2×10^{-5}	6.0×10^{-5}	3.7×10^{-5}

[a] Full formula: $\mathbf{2}^+[B(C_6H_5)_4]^- \cdot 0.1\,C_6H_4F_2$. [b] Full formula: $\mathbf{2}^{2+}[B(C_6H_5)_4]^-_2 \cdot C_6H_4F_2$. [c] $R=\Sigma[(\chi_m T)^{calcd}-(\chi_m T)^{expt}]^2/\Sigma[(\chi_m T)^{expt}]^2$.

$$\chi_m = 2N\beta^2G^2/kT\ \{[\exp(J/kT)]/[1+3\exp(J/kT)]\} + \mathrm{TIP} \quad (1a)$$

$$\chi_m = N\beta^2/4kT\{[g_{1/2}^2 + 10\,g_{3/2}^2\exp(3J/2kT)]/[1+2\exp(3J/2kT)]\} + \mathrm{TIP} \quad (1b)$$

$$\chi_m = 2N\beta^2g^2/kT\{[\exp(J/kT) + 5\exp(3J/kT)]/[1+3\exp(J/kT) + 5\exp(3J/kT)]\} + \mathrm{TIP} \quad (1c)$$

In these expressions the symbols have their usual meanings, $g_{1/2}=(4g_{CrII}-g_{CrI})/3$, $g_{3/2}=(2g_{CrII}-g_{CrI})/3$, and TIP is the temperature-independent paramagnetism. In a first approximation the effects of the single-ion zero-field splitting on the magnetic susceptibility are expected to be negligible. Interestingly, the chromium(II)-containing dinuclear ions $\mathbf{2}^+$ and $\mathbf{2}^{2+}$ have a significantly higher TIP than compound **2**. This indicates more efficient mixing of the ground and excited states in these compounds that may be due to the bigger anisotropy expected for the $S=1$ spin state. The good agreement of the theoretical and experimental magnetic data supports the chosen model. This is noteworthy, because in the lattice stepwise stacking of **2** was observed. From the magnetic data it can be concluded that the π overlap of adjacent molecules is negligibly weak.

The most striking result is that in the given molecular framework of $[[(C_5Me_5)Cr\{[2.2](1,4)cyclophane\}Cr(C_5Me_5)]]^{n+}$ the magnitude of J decreases with increasing number of unpaired electrons. For a qualitative discussion we recall that J is composed of ferro- and antiferromagnetic contributions.[32] In most cases the ferromagnetic contribution is very small, and as we are dealing with negative J values it is neglected here. The antiferromagnetic contribution can be described for a dinuclear compound with isolated spin states S_1 and S_2 by Equation (2).

$$-J = \frac{(\Delta\varepsilon)^2}{4\,S_1S_2(\Delta j)} \quad (2)$$

Here $\Delta\varepsilon$ are the energy differences of the bonding and antibonding combinations of the singly occupied fragment orbitals, and Δj the differences of the two-electron Coulomb integrals. The approach has been worked out in detail by Hay et al.[33] and integrated in an angular overlap approach by Rakitin et al.[34] When according to Equation (2) the J values of Table 1 are plotted against $1/S_1S_2$ a straight line is expected. However, Figure 9 shows some deviation, and

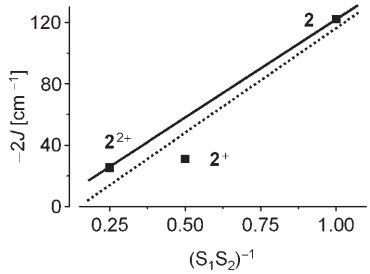

Figure 9. Dependence of the magnetic interaction in $\mathbf{2}^{n+}$ on the number of unpaired electrons. The broken line is the linear-fitting curve; for the solid line, see text.

from the solid line between the values for **2** ($S_1=S_2=1/2$) and $\mathbf{2}^{2+}$ ($S_1=S_2=1$) the drop in the value for the mixed-valent cation $\mathbf{2}^+$ is most obvious. Actually, Equation (2) was defined for molecules in which the metal centers have the same spin state. For mixed-valent compounds additional spin-dependent delocalization (also termed double exchange) must be considered[35] which, simply speaking, is a ferromagnetic contribution and shifts J to more positive values.

The extent to which the magnetic interaction depends on the number of unpaired electrons (i.e., the slope of the solid line in Figure 9) is determined by the interaction across the [2.2](1,4)cyclophane bridge and is summarized in the term $\Delta\varepsilon^2/\Delta j$ of Equation (2). Of course, changes in this term on going from, for instance, **2** to $\mathbf{2}^{2+}$ would modulate the mag-

netic interaction. In any case, the trend of the J values shows that the orbital splittings $\Delta\varepsilon$ resulting from face-to-face interaction of two [(C_5Me_5)Cr(benzene)] molecules play an important role. This is related to the general interest in orbital splittings owing to π-faced interactions.[36] In particular, for cyclophanes it has been shown convincingly by photoelectron spectroscopy[27] that the origin of the splitting is twofold: interaction of the arenes through space and through bonds via hyperconjugation across the ethylene linkers. These contributions cannot be separated with the results presented here because too many orbitals are involved in spin delocalization. According to the NMR and EPR results discussed above, spin is transmitted from the chromium atom to the ligands by direct spin transfer and by polarization. The two singly occupied MOs of compound **2** in Figure 10 show that the ligand content of both and hence direct spin transfer is particularly small. What remains is the spin polarization (of the electrons in eight MOs not shown here) which, like for compound **1**, places much negative spin on the adjacent benzene ring and little positive spin on the distant benzene ring. Since compound **2** has two chromium spin centers this is a mutual process, and each benzene ring receives both positive and negative spin, which is the signature of antiferromagnetic interaction.

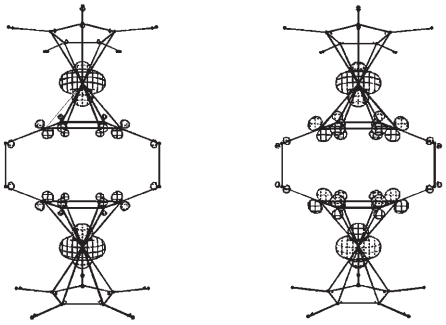

Figure 10. Singly occupied MOs of **2**.

Conclusion

The transfer of a $(C_5Me_5)Cr^{III}$ fragment to [2.2](1,4)cyclophane under reducing conditions can be controlled such that the resulting cyclophane–metal π compounds contain one or two paramagnetic chromium centers (**1** and **2**). According to cyclic voltammetry both compounds can be reduced to chromium(0) species and oxidized to chromium(II) and chromium(III) species. The latter are not stable. The oxidation of **2** proceeds step by step with a potential difference that is typical for electrocommunication and is sufficient for isolating both mixed-valent cation $\mathbf{2}^+$ and dication $\mathbf{2}^{2+}$. In solution $\mathbf{2}^{2+}$ decomposes rapidly by splitting off [2.2](1,4)cyclophane, whose place is taken by one phenyl ring of the tetraphenylborate counterion to give zwitterionic sandwich compound **3**. The NMR spectra show that **3** behaves like chromium sandwiches having two unpaired electrons.

Compound **2** is a triple-decker-like molecule consisting of four π decks, two sandwiched chromium atoms, and a vacancy in the center. Intramolecular interaction between the chromium atoms causes redox splitting, antiferromagnetic coupling, zero-field splitting of the $g_\parallel$ and $g_\perp$ components by $2D$ and D, respectively, as well as a half-field signal in the rigid-solution EPR spectrum. The antiferromagnetic interaction decreases on passing from **2** to $\mathbf{2}^+$, and $\mathbf{2}^{2+}$. This is mainly due to the number of unpaired electrons, which increases from two to three to four, respectively. In addition, double exchange in $\mathbf{2}^+$ weakens the antiferromagnetic interaction.

Spin delocalization from chromium to the ligands is evident from the EPR- and NMR-derived ^{1}H hyperfine coupling constants. The spin density induced in the benzene rings is negative when the chromium spin source is bonded directly and positive when it is remote. Consequently, mutual spin delocalization from the two chromium atoms entails antiferromagnetic interaction. For the design of ferromagnetic interaction it follows that double exchange should be made more efficient and/or one of the (C_5Me_5)Cr fragments of **2** should be replaced by a spin source like the $S=1/2$ (C_5H_5)Fe fragment, for which the sign of the transmitted spin density is inverted.

Experimental Section

All reactions and manipulations were carried out in a nitrogen atmosphere by using Schlenk techniques, oxygen-free and dry solvents, and glassware that was dried at about 140 °C. The elemental analyses were determined by the microanalytical laboratory of the Faculty of Chemistry at Garching.

Mass spectra were obtained from a Varian MAT 311 A instrument. For recording the cyclic voltammograms (CVs) a potentiostat Wenking ST 72, a voltage-scan generator Wenking VSG 72, and a homemade cell consisting of a Pt disk working electrode, a Pt counterelectrode, an Ag/AgCl reference electrode, and a device for drying the solution within the cell immediately before running the CV were available. The compounds were dissolved in a 0.1 M solution of $[n\mathrm{Bu_4N}][PF_6]$ in THF, the concentrations of **1** and **2** were 1.47 mmol L^{-1} and 1.14 mmol L^{-1}, respectively, and the potentials were measured in separate runs after addition of ferrocene relative to the potential of $[Cp_2Fe]/[Cp_2Fe]^+$. At scan rates v between 50 and 800 mV s^{-1} for **1** and between 50 and 400 mV s^{-1} for **2** the ETs to Cr^0 and Cr^{II} proved to be quasireversible, as indicated by an increase of ΔE_p and a decrease of $i_p v^{-1/2}$ with increasing v. All potentials were reproducible within a range of 15 mV or better, and mean values are reported here. For magnetic measurements a Faraday balance was used which consisted of a Bruker B-E 25 C8 magnet, a Sartorius 4102 microbalance, and a low-temperature device. The temperature measurement and adjustment were made with independent Cu/constantan and Au(Fe)/chromel thermocouples. Temperatures below 4.2 K were adjusted by pumping from the helium recipient. All data reported here were measured at 3 kOe. In addition, all samples were measured between 1.3 and 16.2 K at 5, 7, 9, 11, 13, and 15 kOe and gave virtually the same data as at 3 kOe. The diamagnetic corrections for **2**, $\mathbf{2}^+[B(C_6H_5)_4]^-\cdot 0.1\,C_6H_4F_2$, and $\mathbf{2}^{2+}$ $[B(C_6H_5)_4]^-_2\cdot C_6H_4F_2$ were 422, 582, and 835×10^{-6} cm^3 mol^{-1}, respectively. For the EPR spectra an X-band instrument Varian EE 12 was used, and for the NMR spectra a Bruker MSL 300 instrument. The experimental NMR signal shifts δ_T^{expt} at the measuring temperature T were determined

relative to solvent signals; the paramagnetic signal shifts δ_T^{para}, were obtained after calculation relative to corresponding signals of similar diamagnetic compounds ($[(C_5Me_5)_2Fe]$: $\delta(CH_3)=1.70$ ppm, [2.2](1,4)cyclophane:[37] $\delta(C_6H_4)=6.46$ ppm, $\delta(CH_2)=3.06$ ppm, $Na[B(C_6H_5)_4]$:[37] δ(H2/6)=7.20 ppm, δ(H3/5)=6.94 ppm, δ(H4)=6.80 ppm, δ(C1)=164.4 ppm, δ(C2/6)=136.4 ppm, δ(C3/5)=125.2 ppm, δ(C4)=121.4 ppm,), and the final data δ_{305}^{para} were calculated according to the Curie law, which is justified near room temperature, as shown by the magnetic measurements. The paramagnetic signal shifts δ^{para} were converted to hyperfine coupling constants A with Equation (3) by assuming that the dipolar shift contribution to the contact shift is negligible.

$$A = \frac{3\gamma_N kT}{g\beta S(S+1)}\delta_T^{para} \quad (3)$$

Here γ_N is the nuclear gyromagnetic ratio, k the Boltzmann constant, T the absolute temperature, g the electron g factor, β the Bohr magneton, and S the spin quantum number. The Extended Hückel calculations were carried out with the program package CACAO, version 4.0.[38]

(η^5-Pentamethycyclopentadienyl){η^6-[2.2](1,4)cyclophane}chromium (1): A mixture of $AlBr_3$ (13.48 g, 50.5 mmol), $AlCl_3$ (5.03 g, 37.7 mmol), and aluminum powder (2.00 g, 74.1 mmol) was covered with hexane (20 mL) and heated until the aluminum halides had formed a melt. Subsequently, 3.0 mL of a 1.7 M solution of *n*BuLi in hexane were added to destroy traces of protic impurities. After further addition of [2.2](1,4)cyclophane (3.18 g, 15.3 mmol) and $[\{(C_5Me_5)CrCl_2\}_2]$ (3.94 g, 7.6 mmol) the mixture was heated under reflux, whereupon it turned brown. Cooling to ambient temperature, addition of $LiAlH_4$ (4.00 g, 105 mmol), dropwise addition of diethyl ether (20 mL), and stirring for 1 h led to the evolution of H_2 gas. The resulting mixture was diluted with hexane (100 mL), filtered, and the solvents were stripped under reduced pressure. After hexane (10 mL) was added to the solid remainder, a white precipitate was filtered off, and from the red solution the solvent was removed. Recrystallization from diethyl ether (twice) and hexane (once) gave red platelets of **1**; yield 350 mg (5.8% rel. [2.2](1,4)cyclophane). M.p. 170 °C; elemental analysis calcd (%) for $C_{26}H_{31}Cr$ (395.53): C 78.95, H 7.90, Cr 13.15; found: C 78.78, H 8.04, Cr 13.07; MS (EI, 70 eV): *m/z* 395 (52) [M^+], 291 (13) [$(C_5Me_5)Cr(C_8H_8)^+$], 261 (21) [$Cr(C_8H_8)^+$], 208 (23) [$(C_{16}H_{16})^+$], 187 (6) [$(C_5Me_5)Cr^+$], 133 (12) [$(C_5Me_5-2H)^+$], 104, (100) [$(C_8H_8)^+$], 52, (28) [Cr^+], the experimental and theoretical isotope patterns of [M^+] were in agreement; ^{1}H NMR (200 MHz, C_6D_6, 360 K): δ^{exptl} (half-width [Hz])=−9.85 (2300) (30H, CH_3), 0.01 (230) (8H, CH_2), 7.64 (130) (8H, C_6H_4).

Bis(η^5-pentamethycyclopentadienyl)chromium{η^6:η^6-[2.2](1,4)cyclophane} (2): A mixture of [2.2](1,4)cyclophane (1.84 g, 8.8 mmol), $[\{(C_5Me_5)CrCl_2\}_2]$ (7.71 g, 14.9 mmol), $LiAlH_4$ (1.37 g, 36.1 mmol), and 30.0 mL of a 1 M solution of $AlEt_3$ in hexane was first stirred for 15 h at room temperature and then heated at reflux for 30 min. The reaction mixture was allowed to reach room temperature, diluted with diethyl ether 100 mL), and filtered. After stripping the solvents, the remainder was extracted with warm hexane (5×200 mL) and filtered. Removal of the solvent in vacuo gave crystals which were covered with a nonvolatile oil. The crystals were washed with diethyl ether (3×15 mL) and dissolved in THF (300 mL) at 60 °C. After filtration and cooling slowly to room temperature 2.28 g of **2**·THF were obtained as red needles. Another 1.17 g of **2**·THF crystallized after reducing the volume of the mother liquor; overall yield 59.7% (rel. [2.2](1,4)cyclophane). M.p. 250 °C (decomp); elemental analysis calcd (%) for $C_{40}H_{54}Cr_2O$ (654.86): C 73.37, H 8.31, Cr 15.88; found: C 73.39, H 8.31, Cr 15.98. Recrystallization from benzene gave crystals free of solvent. M.p. 230 °C (decomp); elemental analysis calcd (%) for $C_{36}H_{46}Cr_2$ (582.76): C 74.20, H 7.96, Cr 17.84; found: C 73.74, H 7.90, Cr 17.57; MS (EI, 70 eV): *m/z* 395 (0.2) [$M^+-(C_5Me_5)Cr$], 208 (29) [$(C_{16}H_{16})^+$], 104 (100) [$(C_8H_8)^+$]; ^{1}H NMR (200 MHz, C_6D_6, 360 K) δ^{exptl} (half-width [Hz])=−9.02 (2000) (8H, CH_2).

Bis(η^5-pentamethycyclopentadienyl)chromium{η^6:η^6-[2.2](1,4)cyclophane} teraphenyloborate ($2^+[BPh_4]^-$): A solution of **2**·THF (0.6 g, 1.04 mmol) in 1,2-difluorobenzene (15 mL) was cooled to −30 °C and a green suspension of $[(C_5Me_5)_2Fe]^+[B(C_6H_5)_4]^-$ (0.60 g, 0.92 mmol) in 1,2-difluorobenzene (10 mL) was added. While stirring for 15 min at −30 °C a clear red-brown solution formed. Addition of hexane (50 mL) gave a dark precipitate, which was washed with hexane (3×50 mL) and dried in vacuo to yield 0.79 g of a brown microcrystalline powder of $2^+[B(C_6H_5)_4]^-$ (94% rel. $[(C_5Me_5)_2Fe]^+[B(C_6H_5)_4]^-$). The compound decomposed above 150 °C without melting. According to the elemental analysis it contained 0.1 1,2-difluorobenzene per formula unit; elemental analysis calcd (%) for $C_{60}H_{66}Cr_2B\cdot 0.1\,C_6H_4F_2$ (913.40): C 79.68, H 7.32, Cr 11.38, F 0.41; found: C 79.58, H 7.31, Cr 10.80. F 0.38.

Bis(η^5-pentamethycyclopentadienyl)chromium{η^6-[2.2](1,4)cyclophane} bis(tetraphenyloborate) ($2^{2+}[BPh_4]^-_2$): The reaction described in the previous section was carried out with two equivalents of the oxidant: $[(C_5Me_5)_2Fe]^+[B(C_6H_5)_4]^-$ (1.66 g, 2.57 mmol) for **2**·THF (0.89 g, 1.36 mmol). The resulting precipitate was washed with 1,2-difluorobenzene (20 mL) followed by hexane (100 mL) and dried in vacuo to yield $2^{2+}[B(C_6H_5)_4]^-_2$·1,2-difluorobenzene (85% rel. $[(C_5Me_5)_2Fe]^+[B(C_6H_5)_4]^-$) as an orange microcrystalline powder (1.46 g), which decomposed above 150 °C without melting; elemental analysis calcd (%) for $C_{90}H_{90}Cr_2B_2F_2$ (1335.32): C 80.85, H 6.79, Cr 7.79, F 2.85; found: C 80.16, H 6.97, Cr 7.78, F 2.94.

(η^5-Pentamethycyclopentadienyl)(η^6-tetraphenylborate)chromium (3): The salt $[(C_5Me_5)Cr(C_6H_6)]^+[B(C_6H_5)_4]^-$[14] (0.25 g, 0.42 mmol) was shaken in CH_2Cl_2 (10 mL) to give a red solution. When the solution was kept at room temperature for 48 h no color change was visible. Subsequently, CH_2Cl_2 was stripped, the solid was extracted with toluene (100 mL), and the yellow solution was filtered from the remaining solid. After removing toluene under reduced pressure the orange-red residue was dissolved in a few milliliters of THF to give a saturated solution. When the solution was slowly covered with a layer of diethyl ether (25 mL) and allowed to stand for 48 h big red crystals formed which were dried in vacuo. Yield 0.11 g (51%); elemental analysis calcd (%) for $C_{34}H_{35}CrB$ (506.46): C 80.63, H 6.96, Cr 10.26; found: C 80.04, H 7.22, Cr 10.37.

Crystal structure: A crystal of compound **2** was selected, prepared under perfluoropolyether, and mounted in a drop of it onto the tip of a glass fiber on the goniometer head of a Nonius CAD 4 diffractometer. $Mo_{K\alpha}$ radiation, $C_{36}H_{46}Cr_2$, $M_w=582.73\ g\,mol^{-1}$, crystal system orthorhombic, space group $P2_1/c$, $a=10.6242(7)$, $b=12.6047(8)$, $c=11.0229(7)$ Å, $\beta=103.562(9)°$, $V=1434.97(16)$ Å^3, $Z=2$, ρ_{calcd} 1.349 g cm^{-3}, $F(000)=620$, $\mu=0.781$ mm^{-1}, $T=150(2)$ K, θ range 2.49–27.04°. Empirical absorption correction by psi scans ($T_{min/max}=0.65/0.96$). 3477 measured scattering intensities of which 3119 were independent, $R_{int}=0.039$.

The structure was solved by direct methods and refined with the full-matrix least-squares procedure (SHELXTL[21]) against F^2. CCDC-603254 contains the supplementary crystallographic data for this paper. These data can be obtained free of charge from the Cambridge Crystallographic Data Centre via www.ccdc.cam.ac.uk/data_request/cif.

Acknowledgements

We thank Prof. A. A. Pasynskii for helpful discussion and Dr. O. Heigl for growing crystals.

[1] a) L. B. Coleman, M. J. Cohen, D. J. Sandman, F. G. Yamagishi, A. F. Garito, A. J. Heeger, *Solid State Commun.* **1973**, *12*, 1125–1132; b) J. Ferraris, D. O. Cowan, V. Walatka, Jr., J. H. Perlstein, *J. Am. Chem. Soc.* **1973**, *95*, 948–949; c) T. E. Phillips, T. J. Kistenmacher, A. N. Bloch, J. P. Ferraris, D. O. Cowan, *Acta Cryst. Sect. B* **1977**, *33*, 422–428.

[2] a) K. Krogmann, *NATO Advanced Study Institute Series B: Physics*, **1977**, *25*, 225–231; b) J. M. Williams, *Adv. Inorg. Chem. Radiochem.* **1983**, *25*, 235–268.

[3] a) T. J. Marks, *Angew. Chem.* **1990**, *102*, 886–908; *Angew. Chem. Int. Ed. Engl.* **1990**, *29*, 857–879; b) H. Schulz, H. Lehmann, M. Rein, M. Hanack, *Struct. Bonding (Berlin)* **1991**, *74*, 41–146.
[4] a) J. K. Burdett, E. Canadell, *Organometallics* **1985**, *4*, 805–815; b) M. C. Böhm, *Lecture Notes Chem.* **1987**, *45*, 1–181.
[5] a) J. S. Miller, A. J. Epstein, W. Reiff, *Chem. Rev.* **1988**, *88*, 201–220; b) J. S. Miller, *Inorg. Chem.* **2000**, *39*, 4392–4408.
[6] D. W. J. Cruickshank, *Acta Crystallogr.* **1957**, *13*, 504–508.
[7] H. P. Fritz, H. Gebauer, P. Friedrich, P. Ecker, R. Artes, U. Schubert, *Z. Naturforsch. B* **1978**, *33*, 498–506.
[8] H. Bock, C. Arad, C. Näther, Z. Halvas, *J. Chem. Soc. Chem. Commun.* **1995**, 2393–2394.
[9] a) M. Rosenblum, *Adv. Mater.* **1994**, *6*, 159–162; b) R. H. Herber, I. Nowik, M. Rosenblum, *Organometallics* **2002**, *21*, 846–851, and references therein.
[10] Ch. Elschenbroich, M. Wolf, O. Schiemann, K. Harms, O. Burghaus, J. Pebler, *Organometallics* **2002**, *21*, 5810–5819.
[11] P. Jutzi, R. Krallmann, G. Wolf, B. Neumann, H.-G. Stammler, *Chem. Ber.* **1991**, *124*, 2391–2399.
[12] a) J. Schulz, F. Vögtle, *Top. Curr. Chem.* **1994**, *172*, 41–86; b) R. Gleiter, H. Hopf, *Modern Cyclophane Chemistry*, Wiley-VCH, Weinheim, **2004**.
[13] E. O. Fischer, H. P. Kögler, *Z. Naturforsch. B* **1958**, *13*, 197–198.
[14] F. H. Köhler, B. Metz, W. Strauß, *Inorg. Chem.* **1995**, *34*, 4402–4413.
[15] a) W. A. Herrmann, W. R. Thiel, E. Herdtweck, *J. Organomet. Chem.* **1988**, *353*, 323–336; b) A. Grohmann, F. H. Köhler, J. Lachmann, G. Müller, H. Zeh, *Chem. Ber.* **1989**, *122*, 897–899; c) F. H. Köhler, J. Lachmann, G. Müller, H. Zeh, H. Brunner, J. Pfauntsch, J. Wachter, *J. Organomet. Chem.* **1989**, *365*, C15–C18; D. R. Richeson, J. F. Mitchell, K. H. Theopold, *Organometallics* **1989**, *8*, 2570–2577.
[16] a) H. J. Reich, D. J. Cram, *J. Am. Chem. Soc.* **1969**, *91*, 3534–3543; b) A. Venema, N. M. M. Nibbering, T. J. De Boer, *Org. Mass Spectrom.* **1970**, *3*, 1589–1592.
[17] H. Hope, J. Bernstein, K. N. Trueblood, *Acta Crystallogr. B* **1972**, *28*, 1733–1743.
[18] a) Y. Kai, N. Yasuoda, N. Kasai, *Acta Crystallogr. Sect. B* **1982**, *38*, 2840–2843; b) A. de Meijere, O Reiser, M. Stöbbe, J. Kopf, G. Adiwidjaja, V. Sinnwell, S. I. Khan, *Acta Chem. Scand.* **1988**, *42*, 611–625; c) M. D. Ward, P. J. Fagan, J. C. Calabrese, D. C. Johnson, *J. Am. Chem. Soc.* **1989**, *111*, 1719–1732; d) M. Mackawa, N. Hashimoto, T. Kudora-Sowa, Y. Suenaga, M. Manakata, *Inorg. Chim. Acta* **2002**, *328*, 254–258.
[19] a) C. Elschenbroich, F. Gerson, *J. Organomet. Chem.* **1973**, *49*, 445–452; b) J. Heck, G. Rist, *J. Organomet. Chem.* **1988**, *342*, 45–65.
[20] C. Elschenbroich, R. Möckel, U. Zenneck, *Angew. Chem.* **1978**, *90*, 560–561; *Angew. Chem. Int. Ed. Engl.* **1978**, *17*, 531–532.
[21] R. Prins, F. J. Reinders, *Chem. Phys. Lett.* **1969**, *3*, 45–48.
[22] C. Elschenbroich, J. Heck, *J. Am. Chem. Soc.* **1979**, *101*, 6773–6776.
[23] J. R. Pilbrow, *Transition Ion Electron Paramagnetic Resonance*, Clarendon Press, Oxford **1990**, p. 359.
[24] F. B. Bramwell, J. Gendell, *J. Chem. Phys.* **1973**, *58*, 420–427.
[25] F. Gerson, *Top. Curr. Chem.* **1983**, *115*, 57–105.
[26] F. Gerson, H. Ohya-Nishiguchi, C. Wydler, *Angew. Chem.* **1976**, *88*, 617–618; *Angew. Chem. Int. Ed. Engl.* **1976**, *15*, 552–553.
[27] E. Heilbronner, Z.-Z. Yang, *Top. Curr. Chem.* **1983**, *115*, 1–55.
[28] a) W. J. Bowyer, W. E. Geiger, V. Boekelheide, *Organometallics* **1984**, *3*, 1079–1086; b) H. Rabaâ, M. Lacoste, M.-H. Delville-Desbois, J. Ruiz, B. Gloaguen, N. Ardoin, D. Astruc, A. Le Beuze, J.-Y. Saillard, J. Linares, F. Varret, J.-M. Dance, E. Marquestaut, *Organometallics* **1995**, *14*, 5078–5092.
[29] a) R. G. Finke, R. H. Voegeli, E. D. Laganis, V. Boekelheide, *Organometallics* **1983**, *2*, 347–350; b) R. H. Voegeli, H. C. Kang, R. G. Finke, V. Boekelheide, *J. Am. Chem. Soc.* **1986**, *108*, 7010–7016; c) K.-D. Plitzko, B. Rabko, B. Gollas, G. Wehrle, T. Weakley, D. T. Pierce, W. E. Geiger, Jr., R. C. Haddon, V. Boekelheide, *J. Am. Chem. Soc.* **1990**, *112*, 6545–6556.
[30] D. E. Richardson, H. Taube, *Inorg. Chem.* **1981**, *20*, 1278–1285.
[31] B. J. Thomas, S. K. Noh, G. K. Schulte, S. C. Sendlinger, K. H. Theopold, *J. Am. Chem. Soc.* **1991**, *113*, 893–902.
[32] a) O. Kahn, *Molecular Magnetism*, VCH publishers, Weinheim, **1993**, Chapters 8.4.1–8.4.3; b) H. Lueken, *Magnetochemie*, G. B. Teubner, Stuttgart, **1999**, Chapter 5.2.1.
[33] P. J. Hay, J. C. Thibeault, R. Hoffmann, *J. Am. Chem. Soc.* **1975**, *97*, 4884–4899.
[34] Yu. V. Rakitin, S. G. Khodasevich, V. T. Kalinnikov, *Russ. J. Coord Chem.* **1997**, *23*, 13–17.
[35] a) Ref. [32], Chapters 13.2–13.4 and 5.1.2, respectively; b) J. J. Borrás-Almenar, J. M. Clemente-Juan, E. Coronado, A. Palii, B. S. Tsukerblat in *Magnetism: Molecules to Materials, Vol. 1* (Eds.: J. S. Miller, M. Drillon), Wiley-VCH, Weinheim, **2001**, Chapter 5.
[36] a) H.-D. Martin, B. Mayer, *Angew. Chem.* **1983**, *95*, 281–313; *Angew. Chem. Int. Ed. Engl.* **1983**, *22*, 283–314; b) R. Gleiter, W. Schäfer, *Acc. Chem. Res.* **1990**, *23*, 369–375.
[37] National Institute of Advanced Industrial Science and Technology (Japan), data base http://www.aist.go.jp/RIODB/SDBS.
[38] C. Mealli, D. M. Prosperio, *Chem. Educ.* **1990**, *67*, 399–402.

Received: May 23, 2006
Revised: August 8, 2006
Published online: November 6, 2006

